Grain refining and improving mechanical properties of AZ31 Mg alloy sheets by multi-pass warm rolling with falling temperature

Yanchun Zhao
Department of Materials Science and Engineering, Yangze Normal University, Chongqing 408100, China

Hua Zhang,[a] Jianfeng Fan, Lifei Wang, and Qiang Zhang
Key Laboratory of Interface Science and Engineering in Advanced Materials, Ministry of Education, Research Center of Advanced Materials Science and Technology, Taiyuan University of Technology, Taiyuan 030024, China

Cheng Peng
Department of Materials Science and Engineering, Yangze Normal University, Chongqing 408100, China

Hongbiao Dong
Department of Engineering, University of Leicester, Leicester LE1 7RH, U.K.

Bingshe Xu
Key Laboratory of Interface Science and Engineering in Advanced Materials, Ministry of Education, Research Center of Advanced Materials Science and Technology, Taiyuan University of Technology, Taiyuan 030024, China

(Received 20 May 2018; accepted 30 July 2018)

Multi-pass warm rolling with falling temperature was proposed and investigated to obtain AZ31 Mg alloy sheets with a fine-grained microstructure. The results indicated that the grain microstructure of AZ31 alloy sheets was successfully refined from 22.1 to 4.5 μm after multi-pass warm rolling with falling temperature and annealing. Compared to the as-received sheet, the multi-pass warm rolled sheets in annealed condition exhibited weaker (0001) basal texture intensity, which resulted in the significantly increased Schmid factor of $\langle a \rangle$ basal slip. After multi-pass warm rolling with falling temperature, the rolled sheets in annealed condition also exhibited much better mechanical properties, e.g., higher tensile strength, larger fracture elongation, and higher Erichsen value, especially the IE of 8-pass warm rolled sheet in annealed condition was significantly increased by ~33% under the same thickness, which could be attributed to the refined grain microstructure and the weakened basal texture.

I. INTRODUCTION

Magnesium (Mg) and its alloys have promising potential application in the fields of aerospace, automotive, and electronic communication technologies due to their low density, high specific strength, high specific stiffness, high electromagnetic shielding, and so on.[1,2] However, Mg alloys exhibit low strength and ductility because of their hexagonal close packed crystal structure, where limited independent slip systems could be activated at low temperature.[3] Therefore, their wide applications are limited to a great extent. To overcome these defects to improve their mechanical properties at room temperature, extensive efforts are being devoted to microstructural controlling, such as improving texture and grain refinement.[4–6]

A strong (0001) basal texture is usually formed in the traditional rolled or extruded Mg alloys,[7,8] which induces a larger anisotropy and thus deteriorates the stamping formability.[9] Iwanaga et al.[10] significantly enhanced the drawability of Mg alloy sheets at room temperature by weakening the (0001) basal texture. Suh et al.[11] suggested that the drawing depth of the AZ31 Mg sheet could be increased from 6 to 15 mm for the samples before and after equal channel angular pressing (ECAP), which was due to the changing (0001) basal texture. In addition, according to the Hall–Petch relationship, the yield strength (YS) of Mg alloys at room temperature can be dramatically increased by grain refining. Therefore, important efforts have been devoted to refining the grain microstructure of Mg alloys using severe plastic deformation (SPD), e.g., friction stir process,[12,13] different speed rolling,[14,15] cyclic extrusion compression,[16,17] and ECAP.[18,19] Although these SPD processing technologies can fabricate Mg alloys with fine grains even submicron or nanocrystalline grains, they usually possess complicated processes, repeated multiple steps, low efficiency, and high cost. Furthermore, they can only fabricate the material with a small volume and unable to realize the fabrication of large-size Mg alloys.

As one of the important metal plastic processing technologies, rolling has been widely used to produce

[a]Address all correspondence to this author.
e-mail: zhanghua2009@126.com
DOI: 10.1557/jmr.2018.292

 © Materials Research Society 2018

https://doi.org/10.1557/jmr.2018.292 Published online by Cambridge University Press

large-size Mg alloys. The rolling of Mg alloys is usually conducted at elevated temperature due to their poor cold rollability.[20,21] As suggested by Liu et al.,[22] significant grain refinement of Mg alloys was achieved by multi-pass hot rolling, where the grain size was dramatically decreased from 250 μm in ingots to less than 30 μm in the as-rolled sheets. Yu et al.[23] suggested that Mg–Al–Zn–Sn Mg alloy sheets with a fine-grained structure (~5 μm) and tilting (0001) basal texture were prepared by a 16-pass rolling process, thus resulting in the improving mechanical properties. After the AZ61 alloy was symmetrically rolled at a high temperature of 505 °C, the (0001) the basal texture was inclined from the normal direction to the rolling direction and thus the superior formability was obtained.[24] In addition, the temperature control plays a very important role in the hot rolling process of Mg alloy sheets, which dramatically affects the grain size. Chen et al.[25] reported that according to the dependence of grain size on Zener–Hollomon parameter Z ($Z = \dot{\varepsilon}\exp(Q/RT)$, where $\dot{\varepsilon}$ denotes the strain rate, Q denotes the activation energy, R denotes the gas constant, and T denotes the temperature), lowering rolling temperature could dramatically refine the grain size of Mg alloys, especially for multi-pass rolling. Therefore, multi-pass warm rolling with falling temperature was proposed to refine the grain microstructure and improve the mechanical properties in this study. The microstructural evolution of the obtained sheets during rolling and subsequent annealing was investigated, and the corresponding mechanical properties and stretch formability were determined.

II. EXPERIMENT PROCEDURES

In the present work, the as-received AZ31 alloy sheet (rolled and annealed sheet) with a thickness of 3 mm was cut into rectangular samples with dimensions of 100 × 80 mm along the rolling direction. The samples were heated in a furnace at 400 °C for 5 min prior to rolling, and then rolled from 3 to 0.6 mm in thickness by 8-pass rolling with a thickness reduction of about ~80%. Regarding rolling temperature control, after each rolling pass, the rolled samples were returned to the furnace with a decreasing temperature of 20 °C every time and reheated for 5 min. Table I indicates the rolling parameters. After 4, 6, and 8-pass warm rolling with falling temperature, the sheets were rolled to 1.8, 1.2, and 0.6 mm at finish rolling temperatures of 340, 300, and 260 °C, respectively. After multi-pass warm rolling with falling temperature, the rolled sheets were subjected to final annealing at 260 °C for 0.5 h.

TABLE I. Multi-pass warm rolling with falling temperature for AZ31 Mg alloy sheets.

Rolling pass	Finish rolling temperature/°C	Final thickness/mm	Total reduction/%
4	340	1.8	40
6	300	1.2	60
8	260	0.6	80

The optical microstructure was examined by a standard metallographic technique. EBSD measurements were performed on a scanning electron microscope equipped with an EBSD system. EBSD was performed at 20 kV, together with a working distance of 20 mm and a tilt angle of 70 °C. Dog-bone tensile samples with nominal gage dimensions of 10 mm length, 6 mm width, and sheet thickness were machined from the rolled sheets along the angles of 0° (RD), 45, and 90° (TD) to the rolling direction by wire-cutting. Then, uniaxial tensile tests were carried out on a Shimadzu AGX-XD 20kN electronic universal testing machine (Shimadzu Instrument Co. Ltd., Suzhou, China) with a strain rate of 1×10^{-3}/s at room temperature to determine the mechanical properties, e.g., YS, ultimate strength (UTS), and fracture elongation. Each mechanical test was repeated three times to get representative results. Furthermore, the blanks with a square of 55 × 55 mm were machined from the rolled sheets. Standard Erichsen tests were carried out at room temperature using a hemispherical punch having a diameter of 20 mm to investigate the stretch formability of sheets. Here, the punch speed was 2.5 mm/min and the blank-holder force was 10 kN. A graphite grease as a lubricant was pasted only on the center part of the samples. And the Erichsen value (IE), which was the punch stroke at fracture initiation, was measured. Each Erichsen test was also repeated three times to get representative results.

III. RESULTS AND DISCUSSION

A. Microstructural evolution

The optical microstructure of the AZ31 alloy sheets after multi-pass warm rolling with falling temperature are illustrated in Fig. 1. It can be found that the as-received sheet possesses a fully recrystallized equiaxial grain microstructure without twins and the average grain size is about 22.1 μm. After 4-pass warm rolling with falling temperature, the microstructure changed significantly, as shown in Fig. 1(b). The grain boundaries became obscure, a great deal of twins appeared, and individual shear bands together with a small number of recrystallized grains were also observed. While after 6-pass warm rolling with falling temperature, the number of the large grains decreased, but the number of shear bands and recrystallized grains increased obviously [Fig. 1(c)]. As indicated in Fig. 1(d), more shear bands and recrystallized grains were observed after 8-pass warm rolling with falling temperature. Generally, the deformation stored energy of metals is related to the amount of deformation.

https://doi.org/10.1557/jmr.2018.292 Published online by Cambridge University Press

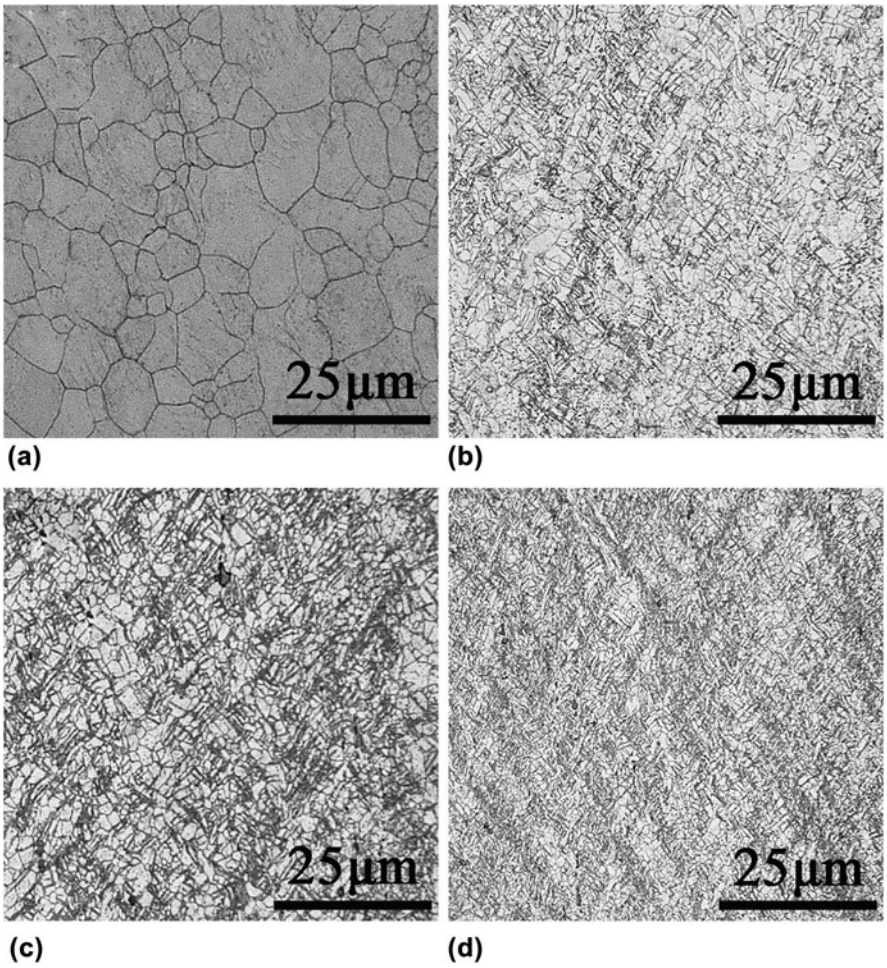


FIG. 1. Optical microstructure of the AZ31 alloy sheets after multi-pass warm rolling with falling temperature: (a) as-received; (b) 4-pass rolled; (c) 6-pass rolled; (d) 8-pass rolled.

The large plastic deformation is usually accompanied by the high deformation stored energy, which favors the recrystallization during subsequent annealing. Recrystallization preferentially develops within shear bands, twins, intersections between grain boundaries and twins, which are the potential nucleation sites for recrystallization.[26,27] This will result in the development of fine recrystallized grains during subsequent annealing.

Figures 2 and 3 show (0001) pole figures, EBSD maps, and Schmid factors of $\langle a \rangle$ basal slip under the loading axis parallel to the RD and TD of various sheets in annealed condition, respectively. According to the reported data,[28] the critical resolved shear stress of basal slip at room temperature is approximately 1/55 that of nonbasal slip, thus Fig. 3 only shows the Schmid factor of $\langle a \rangle$ basal slip. Similar to the result of the optical microstructure, a fully recrystallized equiaxial grain microstructure was observed in the as-received sheet, as shown in Fig. 2(a). In addition, the texture in the as-received sheet is a typical basal texture with the maximum intensity of 17.4, where the *c*-axis of grains is nearly normal to the ND. It is obvious that there is a small Schmid factor of 0.192 or 0.185 for $\langle a \rangle$ basal slip under the loading axis parallel to the RD or TD, which means the poor plasticity for the as-received sheet.

As shown in Figs. 2(b)–2(d), after annealing at 260 °C for 0.5 h, the deformation microstructure of all the rolled sheets changed to a fully recrystallized equiaxial grain microstructure without twins. This is due to the fact that the static recrystallization occurred during the subsequent annealing.[29] As previously mentioned, the nucleation and grain growth occurred preferentially in the shear band twins, intersections between grain boundaries and twins, thus resulting in fine grains after annealing. After 4, 6, and 8-pass warm rolling with falling temperature, the average grain size of the rolled sheets in annealed condition, measured by orientation imaging microscopy software (EDAX Inc., Mahwah, New Jersey), was refined from 22.1 μm to 11.7, 7.4, and 4.5 μm, respectively.

After multi-pass warm rolling with falling temperature, the rolled sheets in annealed condition still exhibited a typical basal texture but the *c*-axis of some grains were

https://doi.org/10.1557/jmr.2018.292 Published online by Cambridge University Press

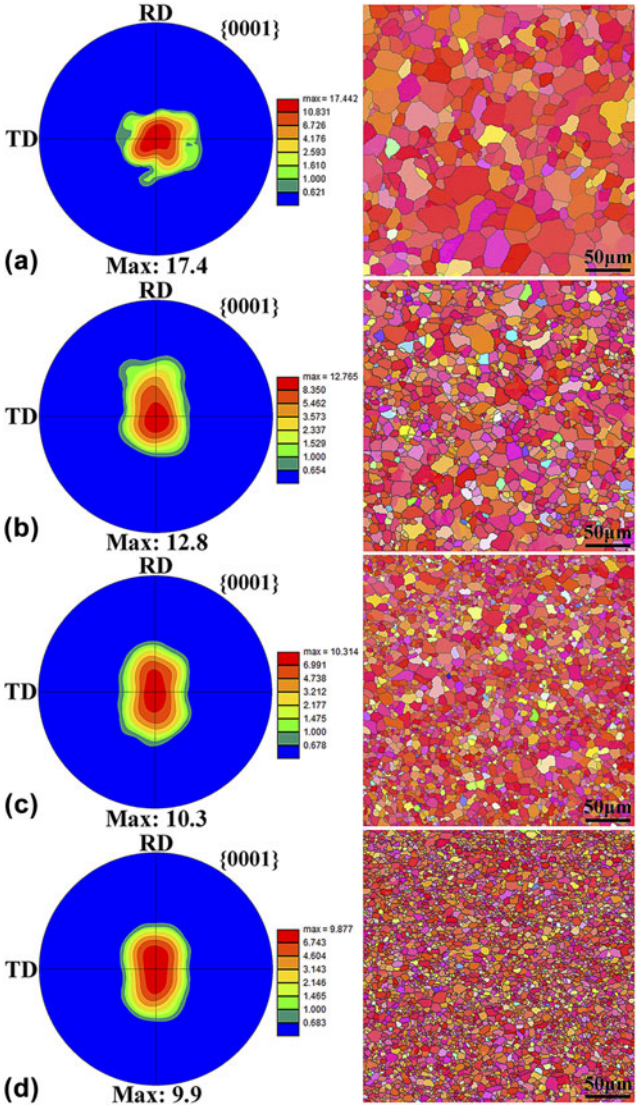


FIG. 2. (0001) pole figures and EBSD maps of various sheets in annealed condition: (a) as-received; (b) 4-pass rolled; (c) 6-pass rolled; (d) 8-pass rolled.

tilted away from the ND towards the RD and lay on the ND-RD plane, thus resulting in the ellipsoidal distribution of basal texture intensity in the (0001) pole figures, as shown in Figs. 2(b)–2(d). This is because the combination of nonbasal slip and twinning leads to the generation of such a texture.[30] Furthermore, compared with the basal texture intensity of the as-received sheet, those of the multi-pass warm rolled sheets in annealed condition were reduced from 17.4 to 12.8, 10.3, and 9.9, respectively, which is due to the increasingly accumulated strain during multi-pass warm rolling. After multi-pass warm rolling with falling temperature and annealing, the soft-oriented grains of $\langle a \rangle$ basal slip are greatly increased due to the weakened basal texture. As indicated in Fig. 3, for the multi-pass warm rolled sheets in annealed condition, the average Schmid factor of

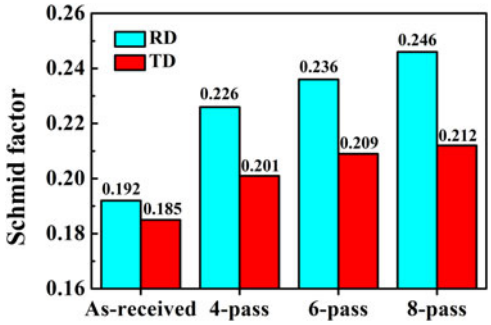


FIG. 3. Schmid factors of $\langle a \rangle$ basal slip under the loading axis parallel to the RD and TD of various passes rolled sheets in annealed condition.

$\langle a \rangle$ basal slip increased from 0.192 to 0.226, 0.236, and 0.246 under the loading axis parallel to the RD, respectively. Under the loading axis parallel to the TD, the average Schmid factor of $\langle a \rangle$ basal slip also increased from 0.185 to 0.201, 0.209, and 0.212 for the multi-pass warm rolled sheets in annealed condition, respectively. This means the plasticity of AZ31 Mg alloy sheets can be effectively improved by multi-pass warm rolling with falling temperature.

B. Mechanical properties

True stress–strain curves of various sheets in annealed condition in different tensile directions at room temperature are presented in Fig. 4. The corresponding mechanical properties, i.e., 0.2% YS, the UTS, and failure elongation (FE) are summarized in Table II, also included are the average grain size, basal texture intensity, and Schmid factor of $\langle a \rangle$ basal slip. For various sheets in annealed condition, the average YS, UTS, and FE in different tensile directions are indicated in Fig. 5. It is clearly observed from the true stress–stain curves in Fig. 4 that for various sheets, the YS depends on the tensile direction due to the influence of the texture,[31] which is a typical characteristic of the conventional rolled AZ31 Mg alloy sheets.[32] It is important to note that all sheets exhibited the lowest YS and the largest fracture elongation in the RD rather than the 45° and TD (Table II and Fig. 4), which can be attributed to the fact that the *c*-axis of some grains inclined from the ND towards the RD during rolling. In addition, the multi-pass warm rolling with falling temperature caused larger yield anisotropy in three different tensile directions, as shown in Figs. 4(b)–4(d). This is because the *c*-axis of some grains became tilted away from the ND towards the RD after multi-pass warm rolling with falling temperature and annealing, as indicated in (0001) pole figures in Fig. 2. As indicated in Table II, after multi-pass warm rolling with falling temperature, the rolled sheets in annealed condition still exhibited higher strength especially the YS regardless of the tensile direction. As shown in Fig. 5,

https://doi.org/10.1557/jmr.2018.292 Published online by Cambridge University Press

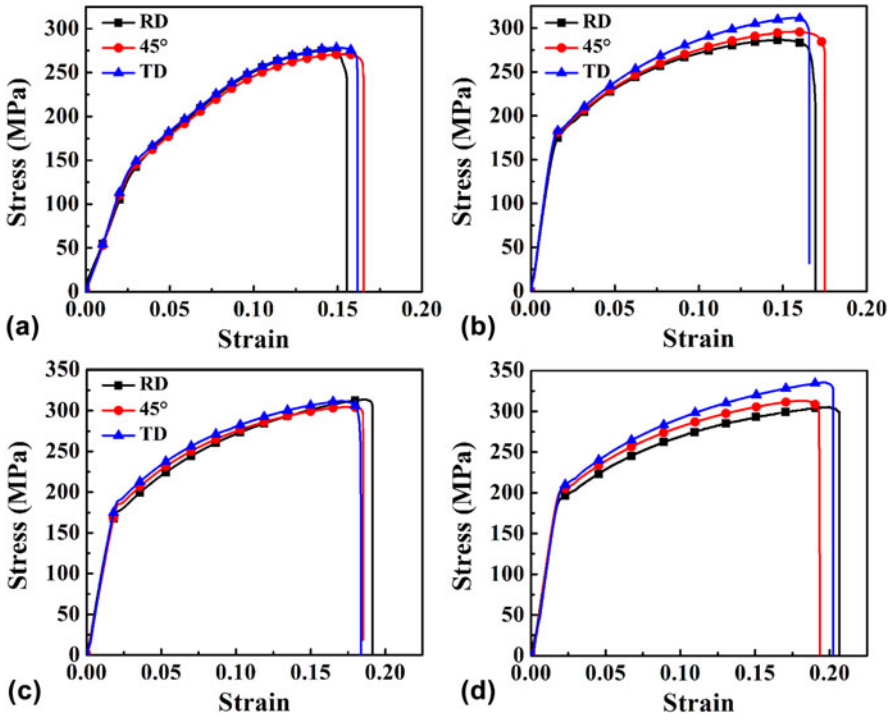


FIG. 4. True stress–strain curves of various sheets in annealed condition in different tensile directions (RD, 45°, TD): (a) as-received; (b) 4-pass rolled; (c) 6-pass rolled; (d) 8-pass rolled.

TABLE II. Mechanical properties of various sheets in annealed condition.

	YS (MPa)			UTS (MPa)			FE (%)				
Sample	RD	45°	TD	RD	45°	TD	RD	45°	TD	Grain size (μm)	Basal texture intensity
As-received	138	140	144	275	271	278	12.8	13.9	13.4	22.1	17.4
4-Pass rolled	168	177	178	286	296	312	15.4	15.9	15.1	11.7	12.8
6-Pass rolled	171	187	189	314	308	312	17.1	16.6	16.5	7.4	10.3
8-Pass rolled	190	200	202	306	313	335	18.8	17.5	18.2	4.5	9.9

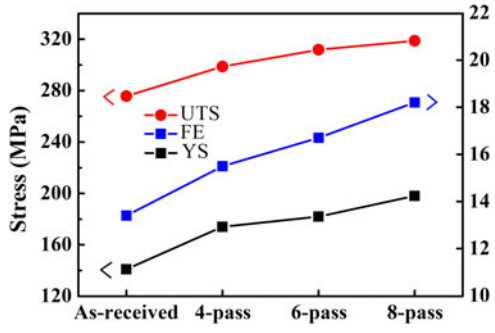


FIG. 5. Average YS, UTS, and FE of various passes rolled sheets in annealed condition in different tensile directions.

the average YS and UTS of the 8-pass warm rolled sheet in annealed condition increased from 141 MPa to 275 MPa of the as-received sheet to 197 MPa and 318 MPa, respectively. According to the Hall–Petch relationship, the increasing strength is mainly due to the grain refinement strengthening resulting from multi-pass warm rolling with falling temperature and annealing. The decrease in grain size will increase the resistance to dislocation motion, and thus resulting in the increasing YS.[33]

As indicated in Table II, after multi-pass warm rolling with falling temperature, the rolled sheets in annealed condition also exhibited larger FE than the as-received sheet in different tensile directions, especially in the RD due to the basal texture becoming more diverse along the RD (Fig. 2). As shown in Fig. 5, the average FE of the 8-pass warm rolled sheet in annealed condition increased from 13.4% of the as-received sample to 18.2%. After multi-pass warm rolling with falling temperature and annealing, the increase in the FE of the AZ31 Mg alloy sheet is ascribed to the larger Schmid factor of $\langle a \rangle$ basal slip resulting from the weakened (0001) basal texture intensity. For Mg alloys with a small Schmid factor of $\langle a \rangle$ basal slip, it is difficult for basal slip system activation during deformation, and accordingly the strain

https://doi.org/10.1557/jmr.2018.292 Published online by Cambridge University Press

localization and premature shear failure are easily produced.[34,35] In addition, the grain refinement can also contribute to the increasing ductility of Mg alloys.[36]

As shown in Fig. 6, the black arrow indicates the macroscopic crack of the Erichsen tested sheet. It is clear that for the as-received sheet with a thickness of 3 mm, the Erichsen value (IE) is very low, only 2.17 mm. The IE of the 8-pass rolled sheet with a thickness of 0.60 mm in annealed condition was dramatically increased to 4.29 mm (increased by ~98%) in comparison to that of the as-received sheet. Considering the thickness of the sheet affecting the stretch formability, the as-received sheet with a thickness of 3 mm was also polished to 0.60 mm to avoid the effect of thickness. After Erichsen testing, the IE of the as-received sheet with a thickness of 0.60 mm is still small, about 3.22, as indicated in Fig. 6 (b). Thus the IE of the 8-pass rolled sheet in annealed condition is still increased by ~33% in comparison to that of the as-received sheet under the same thickness.

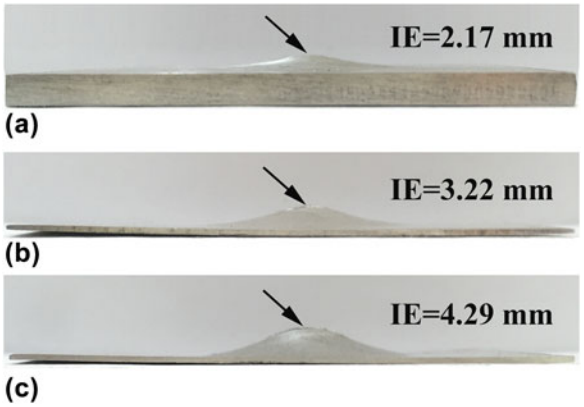


FIG. 6. Erichsen values of (a) as-received sheet, (b) as-received sheet polished to a thickness of 0.60 mm, and (c) 8-pass rolled sheet with a thickness of 0.60 mm in annealed condition.

For the fine-grained microstructure, the amount of deformation can be dispersed in more grains under the same deformation condition to produce homogeneous deformation in each grain without producing serious deformation in a few of grains.[36,37] On the other hand, the finer grains indicate more boundaries, which help to prevent the spread of the crack.[36,37] Therefore, the finer grains can bear larger plastic deformation before the fracture and thus show good plasticity and ductility. In addition, after multi-pass warm rolling with falling temperature and annealing, the improved stretch formability of the AZ31 Mg alloy sheet can also be ascribed to the weakened (0001) basal texture intensity (9.9 versus 17.4), as indicated in Fig. 2. As shown in Fig. 3, the strong basal texture led to a low Schmid factor of $\langle a \rangle$ basal slip in the as-received sheet. The low Schmid factor of $\langle a \rangle$ basal slip indicates that most grains are in an orientation (hard orientation) difficult to deform since the resolved shear stress in the basal plane is equal to zero, and it is difficult to activate the $\langle a \rangle$ basal slip system, which leads to stress localization and premature shear failure.[34,35] Furthermore, for Mg alloys, the strong texture will induce a poor deformation capability of sheet

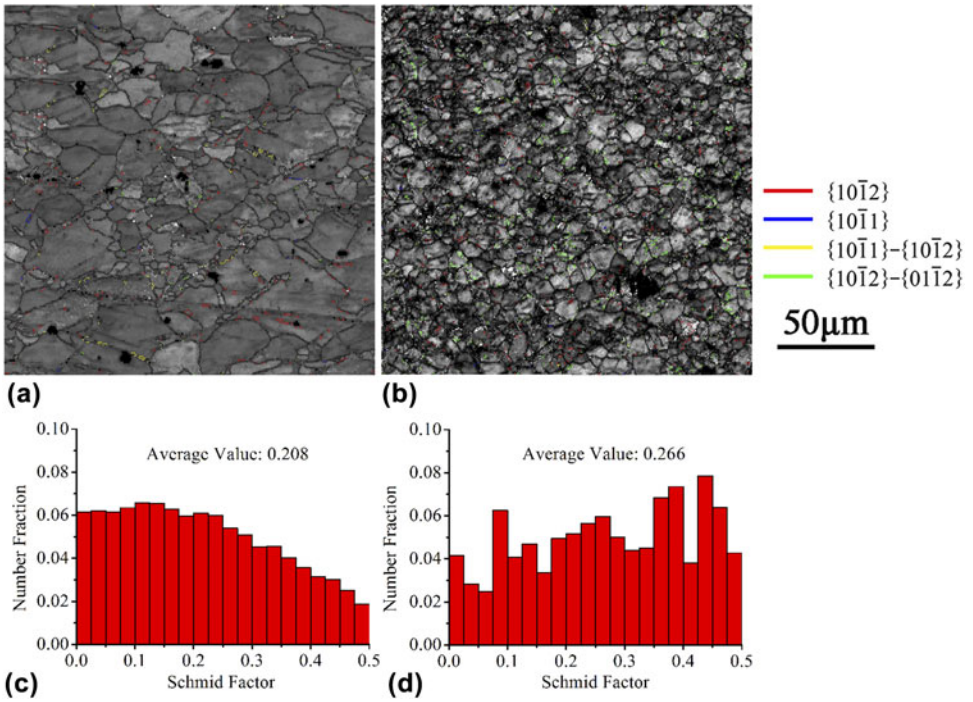


FIG. 7. EBSD maps and Schmid factors of $\langle a \rangle$ basal slip under the loading axis parallel to the RD in the top part of Erichsen tested sheets stretch-formed to failure: (a) and (c) as-received; (b) and (d) 8-pass rolled.

https://doi.org/10.1557/jmr.2018.292 Published online by Cambridge University Press

thinning,[38,39] and consequently resulting in a low ductility at room temperature. Thus, the stretch formability of the AZ31 alloy sheet can also be effectively improved by multi-pass warm rolling with falling temperature.

EBSD maps in the top part of different sheets stretch-formed to failure are indicated in Fig. 7. It is seen from Fig. 7(a) that a small number of twins were observed in the as-received sheet stretch-formed to failure and these twins were judged to be $\{10\bar{1}2\}$, $\{10\bar{1}1\}$ twins and $\{10\bar{1}1\}$–$\{10\bar{1}2\}$ and $\{10\bar{1}2\}$–$\{01\bar{1}2\}$ double twins. Compared to the as-received sheet, more twins and double twins were found in the 8-pass rolled sheet stretch-formed to failure, as shown in Fig. 7(b). It is well known that $\{10\bar{1}2\}$, $\{10\bar{1}1\}$ twins and $\{10\bar{1}1\}$–$\{10\bar{1}2\}$ and $\{10\bar{1}2\}$–$\{01\bar{1}2\}$ double twins will led to grains to rotate by ~86°, 56°, 38°, and 60°, respectively.[40,41] Therefore, the generation of a great number of twins caused lattice rotation and increased the Schmid factor of $\langle a \rangle$ basal slip during stretch deformation, thus resulting in the improved stretch formability. As indicated in Figs. 3 and 7, for the as-received and 8-pass rolled sheets stretch-formed to failure, the Schmid factor of $\langle a \rangle$ basal slip under the loading axis parallel to the RD increased from 0.192 and 0.246 to 0.208 and 0.266, respectively. Furthermore, compared to the as-received sheet stretch-formed to failure, the 8-pass rolled sheet stretch-formed to failure still exhibited larger Schmid factor of $\langle a \rangle$ basal slip (0.266 versus 0.208) under the loading axis parallel to the RD, which contributed to the further deformation during stretch forming and thus enhancing the stretch formability.

IV. CONCLUSION

In summary, multi-pass warm rolling with falling temperature was carried out to investigate its influence on the microstructural evolution and mechanical properties of AZ31 Mg alloy sheets. It is demonstrated that the grain microstructure of AZ31 alloy sheets was successfully refined from 22.1 to 4.5 μm by multi-pass warm rolling with falling temperature and annealing. Multi-pass warm rolling with falling temperature and annealing also produced the weakened (0001) basal texture, which resulted in the significantly increased Schmid factor of $\langle a \rangle$ basal slip. For the 8-pass warm rolled sheet in annealed condition, the average Schmid factor of $\langle a \rangle$ basal slip under the loading axis parallel to the RD or TD increased from 0.192 or 0.185 of as-received to 0.246 or 0.212. Furthermore, due to the refined grain microstructure and the weakened basal texture, the rolled sheets in annealed condition after multi-pass warm rolling with falling temperature exhibited higher tensile strength and larger fracture elongation than the as-received sheet, especially the IE of the 8-pass warm rolled sheet in annealed condition was significantly increased by ~33% under the same thickness.

ACKNOWLEDGMENTS

The authors thank National Natural Science Foundation of China (51504162, U1710118, 51704209, and 51601123), Natural Science Foundation of Shanxi Province (2015011033, 2015021073, and 2016021063), Research Project Supported by Shanxi Scholarship Council of China (2016-029), Shanxi Province Fundamental Resources Platform of Science and Technology (201605D121030), and Scientific and Technological Innovation Programs for Excellent Researchers in Shanxi Province (201605D211015) for their financial supports.

REFERENCES

1. J.C. Li, Z.L. He, P.H. Fu, Y.J. Wu, L.M. Peng, and W.J. Ding: Heat treatment and mechanical properties of a high-strength cast Mg–Gd–Zn alloy. *Mater. Sci. Eng. A* **651**, 745 (2016).
2. W.D. Cui, L. Xiao, W.C. Liu, G.H. Wu, X.F. Wang, and Z.Q. Li: Effect of Zn addition on microstructure and mechanical properties of Mg–9Gd–3Y–0.5Zr alloy. *J. Mater. Res.* **33**, 733 (2018).
3. F.S. Pan, B. Zeng, B. iang, M.X. Zhang, and H.W. Dong: Enhanced mechanical properties of AZ31B magnesium alloy thin sheets processed by on-line heating rolling. *J. Alloys Compd.* **693**, 414 (2017).
4. C.Z. Zhang, S.K. Guan, L.G. Wang, S.J. Zhu, and L. Chang: The microstructure and corrosion resistance of biological Mg–Zn–Ca alloy processed by high-pressure torsion and subsequently annealing. *J. Mater. Res.* **32**, 1061 (2017).
5. J.J. He, B. Jiang, X.W. Yua, J. Xu, Z.T. Jiang, B. Liu, and F.S. Pan: Strain path dependence of texture and property evolutions on rolled Mg–Li–Al–Zn alloy possessed of an asymmetric texture. *J. Alloys Compd.* **698**, 771 (2017).
6. W.L. Cheng, L.F. Wang, H. Zhang, and X.Q. Cao: Enhanced stretch formability of AZ31 magnesium alloy thin sheet by pre-crossed twinning lamellas induced static recrystallizations. *J. Mater. Process. Technol.* **254**, 302 (2018).
7. A. Styczynski, C. Hartig, J. Bohlen, and D. Letzig: Cold rolling textures in AZ31 wrought magnesium alloy. *Scr. Mater.* **50**, 943 (2003).
8. D.L. Yua, D.F. Zhang, J. Sun, Y.X. Luo, J.Y. Xua, H.J. Zhang, and F.S. Pan: Improving mechanical properties of ZM61 magnesium alloy by aging before extrusion. *J. Alloys Compd.* **690**, 553 (2017).
9. S.B. Yi, J. Bohlen, F. Heinemann, and D. Letzig: Mechanical anisotropy and deep drawing behaviour of AZ31 and ZE10 magnesium alloy sheets. *Acta Mater.* **58**, 592 (2010).
10. K. Iwanaga, H. Tashiro, H. Okamoto, and K. Shimizu: Improvement of formability from room temperature to warm temperature in AZ-31 magnesium alloy. *J. Mater. Process. Technol.* **155–156**, 1313 (2004).
11. J. Suh, J. Victoria-Hernández, D. Letzig, R. Golle, and W. Volk: Effect of processing route on texture and cold formability of AZ31 Mg alloy sheets processed by ECAP. *Mater. Sci. Eng. A* **669**, 159 (2016).
12. S. Mironov, T. Onuma, Y.S. Sato, S. Yoneyama, and H. Kokawa: Tensile behavior of friction-stir welded AZ31 magnesium alloy. *Mater. Sci. Eng. A* **679**, 272 (2017).
13. M. Vargas, S. Lathabai, P.J. Uggowitzer, Y. Qi, D. Orlov, and Y. Estrind: Microstructure, crystallographic texture and mechanical behaviour of friction stir processed Mg–Zn–Ca–Zr alloy ZKX50. *Mater. Sci. Eng. A* **685**, 253 (2017).
14. M. Kaseem, B.K. Chung, H.W. Yang, K. Hamad, and Y.G. Ko: Effect of deformation temperature on microstructure and mechanical

https://doi.org/10.1557/jmr.2018.292 Published online by Cambridge University Press

properties of AZ31 Mg alloy processed by differential-speed rolling. *J. Mater. Sci. Technol.* **31**, 498 (2015).
15. D. Luo, H.Y. Wang, L.G. Zhao, C. Wang, G.J. Liu, Y. Liu, and Q.C. Jiang: Effect of differential speed rolling on the room and elevated temperature tensile properties of rolled AZ31 Mg alloy sheets. *Mater. Charact.* **124**, 223 (2017).
16. Q.D. Wang, Y.L. Mu, J.B. Lin, L. Zhang, and H.J. Roven: Strengthening and toughening mechanisms of an ultrafine grained Mg–Gd–Y–Zr alloy processed by cyclic extrusion and compression. *Mater. Sci. Eng. A* **699**, 26 (2017).
17. Y. Tian, H. Huang, G.Y. Yuan, and W.J. Ding: Microstructure evolution and mechanical properties of quasicrystal-reinforced Mg–Zn–Gd alloy processed by cyclic extrusion and compression. *J. Alloys Compd.* **626**, 42 (2015).
18. H. Liu, J. Ju, F.M. Lu, J.L. Yan, J. Bai, J.H. Jiang, and A.B. Ma: Dynamic precipitation behavior and mechanical property of an $Mg_{94}Y_4Zn_2$ alloy prepared by multi-passes successive equal channel angular pressing. *Mater. Sci. Eng. A* **682**, 255 (2017).
19. T. Motoyama, H. Watanabe, N. Ikeo, and T. Mukai: Mechanical and damping properties of equal channel angular extrusion-processed Mg–Ca alloys. *Mater. Lett.* **201**, 144 (2017).
20. Y. Tang, Q.C. Le, W.T. Jia, X. Liu, and J.Z. Cui: Influences of warm rolling and annealing processes on microstructure and mechanical properties of three parent structures containing Mg–Li alloys. *Mater. Sci. Eng. A* **711**, 1 (2018).
21. W.P. Jia, X.D. Hu, H.Y. Zhao, D.Y. Ju, and D.L. Chen: Texture evolution of AZ31 magnesium alloy sheets during warm rolling. *J. Alloys Compd.* **645**, 70 (2015).
22. D. Liu, Z.Y. Liu, and E. Wang: Effect of rolling reduction on microstructure, texture, mechanical properties and mechanical anisotropy of AZ31 magnesium alloys. *Mater. Sci. Eng. A* **612**, 208 (2014).
23. Z.P. Yu, Y.H. Yan, J. Yao, C. Wang, M. Zha, X.Y. Xu, Y. Liu, H.Y. Wang, and Q.C. Jiang: Effect of tensile direction on mechanical properties and microstructural evolutions of rolled Mg–Al–Zn–Sn magnesium alloy sheets at room and elevated temperatures. *J. Alloys Compd.* **744**, 211 (2018).
24. X.S. Huang, K. Suzuki, Y. Chino, and M. Mabuchi: Texture and stretch formability of AZ61 and AM60 magnesium alloy sheets processed by high-temperature rolling. *J. Alloys Compd.* **632**, 94 (2015).
25. W.Z. Chen, W.C. Zhang, L.X. Zhang, and E.D. Wang: Property improvements in fine-grained Mg–Zn–Zr alloy sheets produced by temperature-step-down multi-pass rolling. *J. Alloys Compd.* **646**, 195 (2015).
26. X. Li, P. Yang, L.N. Wang, L. Meng, and F. Cui: Orientational analysis of static recrystallization at compression twins in a magnesium alloy AZ31. *Mater. Sci. Eng. A* **517**, 160 (2009).
27. M.M. Myshlyaev, H.J. McQueen, A. Mwembela, and E. Konopleva: Twinning, dynamic recovery and recrystallization in hot worked Mg–Al–Zn alloy. *Mater. Sci. Eng. A* **337**, 121 (2002).
28. M. Suzuki, H. Sato, K. Maruyama, and H. Oikawa: Creep deformation behavior and dislocation substructures of Mg–Y binary alloys. *Mater. Sci. Eng., A* **319–321**, 751 (2001).
29. X. Huang, K. Suzuki, and Y. Chino: Annealing behaviour of Mg–3Al–1Zn alloy sheet obtained by a combination of high-temperature rolling and subsequent warm rolling. *J. Alloys Compd.* **509**, 4854 (2011).
30. Y. Chino, K. Kimura, and M. Mabuchi: Twinning behavior and deformation mechanisms of extruded AZ31 Mg alloy. *Mater. Sci. Eng. A* **483**, 481 (2008).
31. Q.S. Yang, B. Jiang, G.Y. Zhou, J.H. Dai, and F.S. Pan: Influence of an asymmetric shear deformation on microstructure evolution and mechanical behavior of AZ31 magnesium alloy sheet. *Mater. Sci. Eng. A* **590**, 440 (2014).
32. D.W. Brown, S.R. Agnew, M.A.M. Bourke, T.M. Holden, S.C. Vogel, and C.N. Tomé: Internal strain and texture evolution during deformation twinning in magnesium. *Mater. Sci. Eng. A* **399**, 1 (2005).
33. H. Zhang, W.L. Cheng, J.F. Fan, B.S. Xu, and H.B. Dong: Improved mechanical properties of AZ31 magnesium alloy sheets by repeated cold rolling and annealing using a small pass reduction. *Mater. Sci. Eng. A* **637**, 243 (2015).
34. S.R. Agnew and O. Duygulu: A mechanistic understanding of the formability of magnesium: Examining the role of temperature on the deformation mechanisms. *Mater. Sci. Forum* **419–422**, 177 (2003).
35. S.R. Agnew and O. Duygulu: Plastic anisotropy and the role of non-basal slip in magnesium alloy AZ31B. *Int. J. Plast.* **21**, 1161 (2005).
36. J.A. del Valle, F. Carreño, and O.A. Ruano: Influence of texture and grain size on work hardening and ductility in magnesium-based alloys processed by ECAP and rolling. *Acta Mater.* **54**, 4247 (2006).
37. W. Yuan and R.S. Mishra: Grain size and texture effects on deformation behavior of AZ31 magnesium alloy. *Mater. Sci. Eng. A* **558**, 716 (2012).
38. H. Zhang, G.S. Huang, L.F. Wang, and J.H. Li: Improved formability of Mg–3Al–1Zn alloy by pre-stretching and annealing. *Scr. Mater.* **67**, 495 (2012).
39. J. Koike, T. Kobayashi, T. Mukai, H. Watanabe, M. Suzuki, K. Maruyama, and K. Higashi: The activity of non-basal slip systems and dynamic recovery at room temperature in fine-grained AZ31B magnesium alloys. *Acta Mater.* **51**, 2055 (2003).
40. M.R. Barnett: Twinning and the ductility of magnesium alloys: Part I: "Tension" twins. *Mater. Sci. Eng. A* **464**, 1 (2007).
41. M.R. Barnett: Twinning and the ductility of magnesium alloys: Part II. "Contraction" twins. *Mater. Sci. Eng. A* **464**, 8 (2007).

https://doi.org/10.1557/jmr.2018.292 Published online by Cambridge University Press